

Numerical approximation of the Voigt regularization of incompressible NSE and MHD flows

Paul Kuberry * Adam Larios † Leo G. Rebholz‡ Nicholas E. Wilson§

June 12, 2012

Abstract

We study the Voigt-regularizations for the Navier-Stokes and MHD equations in the presence of physical boundary conditions. We develop the first finite element numerical algorithms for these systems, prove stability and convergence of the algorithms, and test them on problems of practical interest. It is found that unconditionally stable implementations of the Voigt regularization can be made from a simple change to existing NSE and MHD codes, and moreover, optimal convergence of the developed algorithms' solutions to physical solutions can be obtained if lower order mixed finite elements are used. Finally, we show that for several test problems, the Voigt regularization produces good coarse mesh approximations to NSE and MHD systems; that is, the Voigt regularization provides accurate reduced order models for NSE and MHD flows.

1 Introduction

In this paper, we investigate numerically and computationally the Voigt regularization of the incompressible Navier-Stokes equations (NSE) for fluid flow, and the magnetohydrodynamic (MHD) equations for the flow of fluids with electromagnetic properties. This inviscid regularization was first introduced and studied by A. P. Oskolkov in [25] as a model for certain viscoelastic fluids known as Kelvin-Voigt fluids, and was later proposed as a regularization for the Navier-Stokes equations by Y. Cao, E. Lunasin, and E. S. Titi in [2] as a smooth, inviscid regularization of the 2D and 3D Navier-Stokes equations for the purpose of direct numerical simulations (DNS). The Voigt regularization of the incompressible NSE is given in dimensionless form by the system

$$-\alpha_1^2 \Delta u_t + u_t - Re^{-1} \Delta u + u \cdot \nabla u + \nabla p = f, \quad (1.1a)$$

$$\nabla \cdot u = 0, \quad (1.1b)$$

$$u(0) = u^0, \quad (1.1c)$$

with appropriate boundary conditions, discussed below. Here, u represents velocity of the fluid, p the pressure, f a given body force, and $Re > 0$ is the Reynolds number. $\alpha_1 > 0$ is

*Department of Mathematical Sciences, Clemson University, Clemson, SC 29634, pkuberr@clemson.edu.

†Department of Mathematics, Texas A&M University, College Station, TX 77843, alarios@math.tamu.edu, <http://www.math.tamu.edu/~alarios>

‡Department of Mathematical Sciences, Clemson University, Clemson, SC 29634, rebholz@clemson.edu, <http://www.math.clemson.edu/~rebholz>. Partially supported by National Science Foundation grants DMS0914478 and DMS1112593.

§Department of Mathematical Sciences, Clemson University, Clemson, SC 29634, newilso@clemson.edu. Partially supported by National Science Foundation grant DMS0914478.

a dimensionless regularization parameter. (We note that, in the dimensional version, the regularizing parameter α_1 has units of length.) Notice that by formally setting $\alpha_1 = 0$, one recovers the usual NSE. The NSE-Voigt model is of particular interest as it is the only known regularization of Navier-Stokes equations which is known to be globally well-posed in the case of Dirichlet (i.e., no-slip) boundary conditions. To the best of our knowledge, all other regularizations of the NSE require additional, non-physical boundary conditions to be applied. We also study a Voigt regularization of the MHD equations, where a Voigt-term is used in both the momentum and magnetic equations, see (4.1) (we refer to this system as the MHD-Voigt model).

The major contribution of this work is the computational testing of NSE-Voigt, and the algorithm development, numerical analysis, and computational testing for MHD-Voigt. The present work represents the first numerical and computational studies of the MHD-Voigt regularization. For NSE-Voigt, we will see that once it is discretized, it has the distinct flavor of eddy viscosity type models studies in [16] and [8], and in fact for the proposed NSE-Voigt algorithm, an identification of NSE-Voigt regularization parameters with the eddy-viscosity stabilization parameters in [16] will directly prove the stability and convergence of our algorithm. Hence the main contribution for NSE-Voigt is the connection to the known algorithms, and the testing of it on a benchmark problem more complex than laminar flow around a cylinder as done in [16],[8].

System (1.1) was shown to be globally well-posed in [25, 26] in the case $Re < \infty$. Later, in [2] the case $Re = \infty$ was studied (under periodic boundary conditions), and it was shown that in this case (1.1) is globally well-posed, backwards and forward in time. Furthermore, the following modified energy equality was rigorously proven (with Re being either finite or infinite):

$$\|u(t)\|_{L^2(\Omega)}^2 + \alpha_1^2 \|\nabla u(t)\|_{L^2(\Omega)}^2 + Re^{-1} \int_0^t \|\nabla u(s)\|_{L^2(\Omega)}^2 ds = \|u^0\|_{L^2(\Omega)}^2 + \alpha_1^2 \|\nabla u^0\|_{L^2(\Omega)}^2. \quad (1.2)$$

The equations (1.1) in the case $Re = \infty$ are sometimes called the Euler-Voigt equations. It is worth noting that, to the best of our knowledge, the Voigt-regularization is the only known inviscid regularization of the Euler equations for which global existence is established. Higher-order regularity in Sobolev spaces, as well as a Gevrey class (spatial analytic) regularity were proven in [17]. It was also shown in [17] that, given the same (sufficiently smooth) initial data, solutions to the NSE-Voigt [resp. Euler-Voigt] equations converge to solutions of the NSE [resp. Euler-Voigt] as $\alpha_1 \rightarrow 0$, and a new criterion for blow-up of solutions to the NSE [resp. Euler] equations, based on the Voigt-regularization, was established. For a numerical investigation of the Euler-Voigt equations, see [19].

The statistical properties of the NSE-Voigt model were investigated computationally, using a phenomenological model of turbulence known as the Sabra shell model, in [21]. It was observed that, for values of α_1 which were smaller than (the Sabra-shell analogue of) the Kolmogorov dissipation length scale, the structure functions of second, third, and fourth order for the NSE and the NSE-Voigt model obey the same power law in the inertial range. For values of α_1 larger than the Kolmogorov scale, it was observed in [21] that two distinct regions related to the inertial range of the energy spectrum arise. In particular, in the low wave-numbers a region obeying the Kolmogorov $k^{2/3}$ power law was observed, while in the high wave-numbers, there appears to be a region where energy condensates.

The MHD-Voigt model was first introduced and studied in [17], where global well-posedness was established in the 3D periodic case, even with zero fluid viscosity and zero magnetic resistivity. A similar model with Voigt-regularization only on the momentum

equation, but with non-zero magnetic resistivity, was studied in [5, 18]. Similar to the case of the NSE-Voigt system, it has also been noted in [18] that the 3D MHD-Voigt system (with non-zero viscosity and magnetic resistivity) is globally well-posed under physical boundary conditions. In the same light as the Euler-Voigt equations, convergence as the regularizing parameter $\alpha_1 \rightarrow 0$, as well as a blow-up criterion for the MHD system, based on the regularization, have been established in [18].

This paper is organized as follows. Section 2 presents notation and preliminaries for a smoother analysis to follow in later sections. In Section 3, we introduce a finite element algorithm to solve the NSE-Voigt system, which we observe to be closely related to eddy viscosity type models studied in [16] and [8]. Through this connection to existing literature and an identification of parameters, we can immediately conclude stability and convergence of our algorithm. We then successfully test the algorithm on a test problem from [15]. In Section 4, we propose a numerical scheme for the MHD-Voigt equations. A thorough stability and convergence analysis for this scheme is carried out in Subsection 4.1, and in Subsection 3.1, we consider two test cases for the MHD-Voigt equations: channel flow over a step, and the Orszag-Tang vortex problem. In both cases, the Voigt regularization is shown to give good coarse mesh approximations to the physical solution.

2 Notation and Preliminaries

We consider a domain $\Omega \subset \mathbb{R}^d$ ($d = 2$ or 3), with Dirichlet boundary conditions for both velocity and the magnetic field. For simplicity of exposition, we consider the case of a convex polyhedral domain and homogeneous Dirichlet conditions, but the extension to other cases can be done in the usual way [28].

We will denote the $L^2(\Omega)$ norm and inner product by $\|\cdot\|$ and (\cdot, \cdot) , respectively. The $L^\infty(\Omega)$ norm will be denoted by $\|\cdot\|_\infty$ and $H^k(\Omega)$ norms by $\|\cdot\|_k$. All other norms will be clearly labeled.

The Poincaré-Freidrich's inequality will be used throughout our analysis: For $\phi \in H_0^1(\Omega)$,

$$\|\phi\| \leq C(\Omega) \|\nabla \phi\|.$$

The following lemma for bounding the trilinear forms will be used often in our analysis.

Lemma 2.1. *For $u, v, w \in H_0^1(\Omega)$, there exists $C = C(\Omega)$ such that*

$$(u \cdot \nabla v, w) \leq C \|\nabla u\| \|\nabla v\| \|w\|^{1/2} \|\nabla w\|^{1/2} \quad (2.1)$$

$$(u \cdot \nabla v, w) \leq C \|\nabla u\| \|\nabla v\| \|\nabla w\| \quad (2.2)$$

Proof. These estimates follow from Hölder's inequality, the Sobolev imbedding theorem and Poincare-Freidrich's inequality. \square

We denote by τ_h a regular, conforming mesh of Ω with maximum element diameter h . The finite element spaces used throughout will be the Scott-Vogelius (SV) pair, $(X_h, Q_h) = ((P_k)^d, P_{k-1}^{disc})$ will approximate velocity and pressure, as well as the magnetic field and corresponding Lagrange multiplier in the MHD case, where P_k denotes a continuous piecewise polynomials that are degree k on each element, and P_{k-1}^{disc} denotes a discontinuous approximation space consisting of piecewise polynomials of degree $k - 1$ on each element. SV elements provide point-wise enforcement of the divergence free constraints even though finite element schemes enforce it only weakly. This property makes it an attractive choice

for NSE and MHD models that are wished to be used on coarse meshes, since here the weak enforcement of mass conservation can be a big problem [3, 4, 22]. It is also attractive for MHD, since there are two solenoidal constraints, and their strong enforcement can dramatically improve solutions [4]. Specifying this choice of elements leads to some simplification of the analysis, since the nonlinear terms do not require skew symmetrization for stability, but extension of these results to other common element choices such as $((P_k)^d, P_{k-1})$ Taylor-Hood can be done with minimal effort, and with nearly identical results.

The use of SV elements requires a mesh restriction for inf-sup stability and optimal approximation properties. If $k \geq d$, then it is sufficient that the mesh be created as a barycenter refinement of a regular mesh [27, 30]. Our computations will satisfy this requirement, although there are different types of meshes and polynomial degrees for which SV elements can be stable (see, e.g., [31, 32, 33]).

As alluded to above, a fundamentally important property of Scott-Vogelius elements is that the usual finite element weak enforcement of incompressibility, via

$$(\nabla \cdot v_h, q_h) = 0 \quad \forall q_h \in Q_h,$$

enforces incompressibility point-wise, since q_h can be chosen as $q_h = \nabla \cdot v_h$ since $\nabla \cdot X_h \subset Q_h$, thus providing

$$\|\nabla \cdot v_h\|^2 = 0 \implies \nabla \cdot v_h = 0.$$

We define the space of discretely divergence free function as

$$V_h := \{v_h \in X_h : (\nabla \cdot v_h, q_h) = 0 \quad \forall q_h \in Q_h\}.$$

In light of the above equations, when using SV elements, functions in V_h are point-wise divergence free.

The following well known lemma from [14] will be used in the MHD convergence analysis.

Lemma 2.1. (*Discrete Grönwall Lemma*) Let Δt , H and a_n, b_n, c_n, d_n be nonnegative numbers such that for $M \geq 0$

$$a_M + \Delta t \sum_{n=0}^M b_n \leq \Delta t \sum_{n=0}^M d_n a_n + \Delta t \sum_{n=0}^M c_n + H.$$

Furthermore, suppose that the time step satisfies $\Delta t d_n < 1$ for each n . Then,

$$a_M + \Delta t \sum_{n=0}^M b_n \leq \exp \left(\Delta t \sum_{n=0}^M d_n \right) \left(\Delta t \sum_{n=0}^M c_n + H \right).$$

3 A finite element algorithm for NSE-Voigt

The numerical scheme we propose for approximating solutions to (1.1a)-(1.1b) is a Galerkin finite element spatial discretization and linear extrapolated (via Baker's method [1]) trapezoidal time discretization. Denote $u_h^{n+\frac{1}{2}} := \frac{1}{2}(u_h^n + u_h^{n+1})$. We require the discrete initial conditions to be point-wise divergence free, that is, $u_h^0 \in V_h$, and define $u_h^{-1} := u_h^0$. Then the scheme reads as follows: $\forall (v_h, q_h) \in (X_h, Q_h)$ find $(u_h^{n+1}, p_h^{n+\frac{1}{2}}) \in (X_h, Q_h)$ for

$$n = 0, 1, 2, \dots, M = \frac{T}{\Delta t}$$

$$\frac{1}{\Delta t}(u_h^{n+1} - u_h^n, v_h) + \frac{\alpha_1^2}{\Delta t}(\nabla(u_h^{n+1} - u_h^n), \nabla v_h) + ((\frac{3}{2}u_h^n - \frac{1}{2}u_h^{n-1}) \cdot \nabla u_h^{n+\frac{1}{2}}, v_h)$$

$$+ Re^{-1}(\nabla u_h^{n+\frac{1}{2}}, \nabla v_h) - (p_h^{n+\frac{1}{2}}, \nabla \cdot v_h) = (f(t^{n+\frac{1}{2}}), v_h) \quad (3.1)$$

$$(\nabla \cdot u_h^{n+1}, q_h) = 0 \quad (3.2)$$

The finite element scheme (3.1)-(3.2) for NSE-Voigt is identical to an NSE scheme with an eddy viscosity type stabilization term, studied by Layton et al. in [16], if we make the identification of the coefficients of the Voigt term with the stabilization term, i.e. $\alpha_1^2/\Delta t = ch$, where c is an order 1 constant and h is the max element diameter. The work in [16] provided a numerical analysis of the scheme and a benchmark test of 2D flow around a cylinder that showed the stabilization term can help provide better coarse mesh approximations than without the term. The key numerical analysis results are as follows, after changing the stabilization coefficient to be the Voigt coefficient.

We note that if one has a Crank-Nicolson NSE code already, the only changes necessary to convert to NSE-Voigt are to change the viscous terms' coefficients by a constant.

Lemma 3.1. *(Unconditional stability) Suppose $f \in L^2(0, T; H^{-1}(\Omega))$. Then the scheme (3.1)-(3.2) is unconditionally stable: for any $\Delta t > 0$, solutions to the scheme satisfy*

$$\|u_h^M\|^2 + \alpha_1^2 \|\nabla u_h^M\|^2 + Re^{-1} \Delta t \sum_{n=0}^{M-1} \|\nabla u_h^{n+1/2}\|^2 \leq C(u_0, f, Re, T).$$

Since the scheme is linear and finite dimensional at each time step, analysis similar to that used in the stability estimate can be used to show that solutions at each time step are unique, and therefore exist uniquely.

A convergence result for the scheme is proven in [16], which gives an optimal result for a convergence estimate that uses mixed finite elements with trapezoidal time stepping and a $O(\alpha_1^2)$ stabilization term. The result is proven for Taylor-Hood elements and an $O(h)$ coefficient on the stabilization term, but can be trivially extended for SV elements and a stabilization term with coefficient $\alpha_1^2/\Delta t$, and reads:

Theorem 3.1. *Suppose (u, p) is a strong solution to the NSE on $\Omega \times [0, T]$ satisfying $u \in L^2(0, T; H^{k+1}(\Omega))$, $u_t \in L^2(0, T; H^{k+1}(\Omega))$, $u_{tt} \in L^\infty(0, T; H^2(\Omega))$, $u_{ttt} \in L^\infty(0, T; L^2(\Omega))$, and the mesh width h and time step Δt are chosen sufficiently small so that we have $\|u\|_{L^\infty(0, T; H^{k+1}(\Omega))} \Delta t h^{k-d/2} \leq C(\text{data}) \approx O(1)$. Then*

$$\|u(T) - u_h^M\| + \left(\Delta t Re^{-1} \sum_{n=0}^{M-1} \|\nabla u(t^{n+1/2}) - \nabla u_h^{n+1/2}\|^2 \right)^{\frac{1}{2}} \leq C \left(h^k + \alpha_1^2 + \Delta t^2 \right).$$

Remark 3.1. *The convergence estimate suggests that optimal accuracy of the scheme to an NSE solution can be achieved (in the asymptotic sense in the energy norm) if $\alpha_1 \leq C \max\{\Delta t, h^{k/2}\}$. Hence in the most common case of $k = 2$, the choice of $O(h)$ for the regularization parameter will provide optimal accuracy.*

We now present a numerical test for the NSE-Voigt scheme on a test problem that is more complex than those performed in [16].

3.1 A numerical test for NSE-Voigt

The numerical test we study is a channel flow problem with a contraction and two outlets. To the best of our knowledge, this problem was first tested by Turek et al. in [15], and is very challenging since there are several possible sources of numerical instability. The domain is a 1 inlet, 2 outlet channel, with a smooth contraction. A diagram of the domain is given in Figure 1.

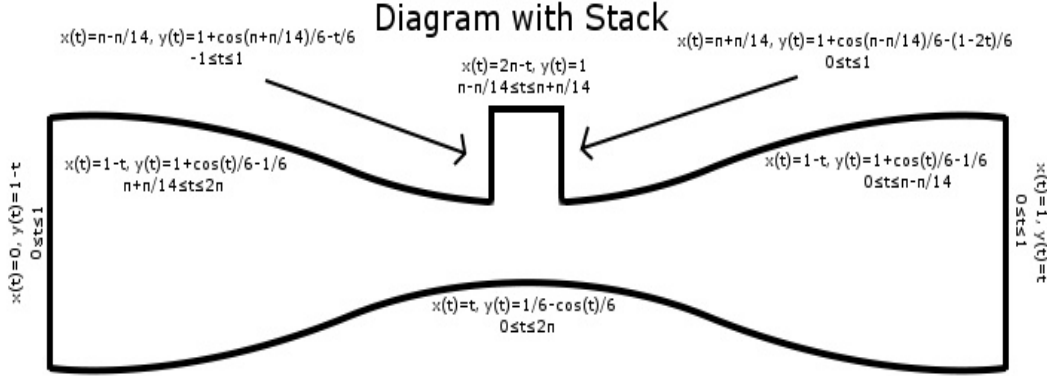


Figure 1: Shown above is a diagram of the NSE-Voigt test problem

The inflow boundary condition was enforced to have a parabolic profile with max velocity $u_{inlet}^{max} = 1$. At the two outlets, zero mean stress conditions were enforced, which were implemented as ‘do-nothing’ conditions. On the rest of the boundary, homogeneous Dirichlet conditions were enforced for the velocity. We took the Reynolds number $Re=1,000$, and started the flow from rest at $T=0$, and ran it out to $T=4$.

For this experiment, we used (P_2, P_1^{disc}) Scott-Vogelius elements, with a barycenter refined triangular mesh (a sufficient stability condition for Scott-Vogelius elements to be inf-sup stable). These mixed finite elements have the attractive property that discrete velocity solutions are point-wise divergence-free, which is an important property for certain types of flows [3, 22]. In particular, for this test example, we also tested with (P_2, P_1) Taylor-Hood elements and got very poor results without a very strong L^2 penalization of the divergence with grad-div stabilization. Hence, it seems Scott-Vogelius elements are a natural choice for this problem.

The meshes used in the computations are shown in Figure 2. The coarse mesh provides 11,758 total degrees of freedom (dof), and the fine mesh provides 99,992 total dof. We compute the NSE on the fine mesh (with $\alpha = 0$) using (3.1)-(3.2) and time step $\Delta t = 0.01$, and believe this solution as the truth solution (based on numerous other computations on several other meshes and time steps). Plots of the fine mesh velocity solution at $T=1, 2, 3$ and 4 are shown in Figure 3, as speed contours.

The goal of the model we study is to produce good approximations to the solution, but using significantly fewer degrees of freedom than is required by a direct simulation with the NSE. Hence we run (3.1)-(3.2) on the coarse mesh with parameter $\alpha = 0.1 \approx h$, and for comparison, we also run the usual NSE (i.e. ‘no model’ or, equivalently, the model with $\alpha = 0$) on the same coarse mesh. Results for $T=1, 2, 3$, and 4 are shown in Figure 4 for the coarse mesh NSE and in Figure 5 for NSE-Voigt. We observe that on the coarse mesh, the

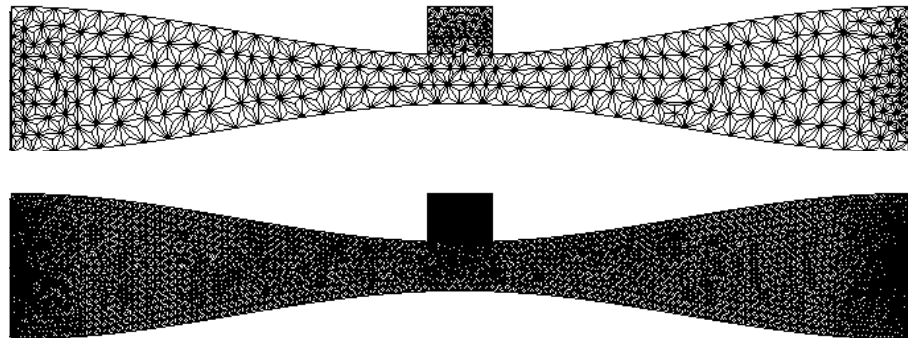


Figure 2: Shown above are the meshes used in the numerical experiment for approximating NSE flows.

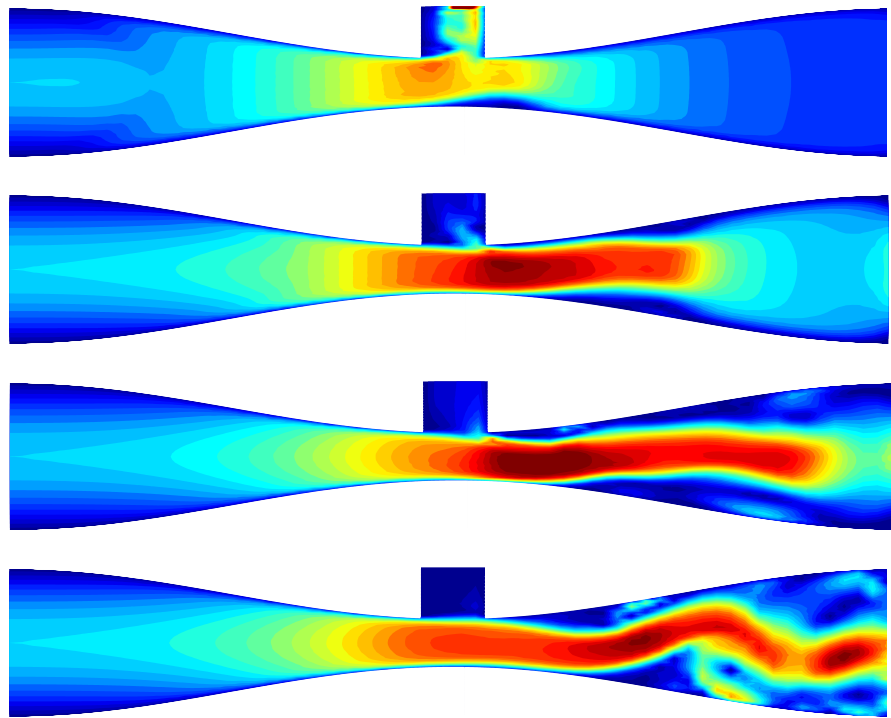


Figure 3: Shown above is the fine mesh NSE solution at $T=1,2,3,4$, from top to bottom, displayed as speed contours.

usual NSE is under-resolved, and significant numerical oscillations are present. Moreover, by $T=4$, the overall flow pattern of the coarse mesh NSE solution does not match the fine mesh NSE solution on the right hand side of the contraction; the fine mesh solution is turning ‘up’ at the outflow, while the coarse mesh solution does not predict this behavior. On this same coarse mesh, the NSE-Voigt model’s solution has only very minor oscillations, and predicts the overall flow pattern very well at $T=1, 2, 3$, and 4. Hence this is a successful test for NSE-Voigt.

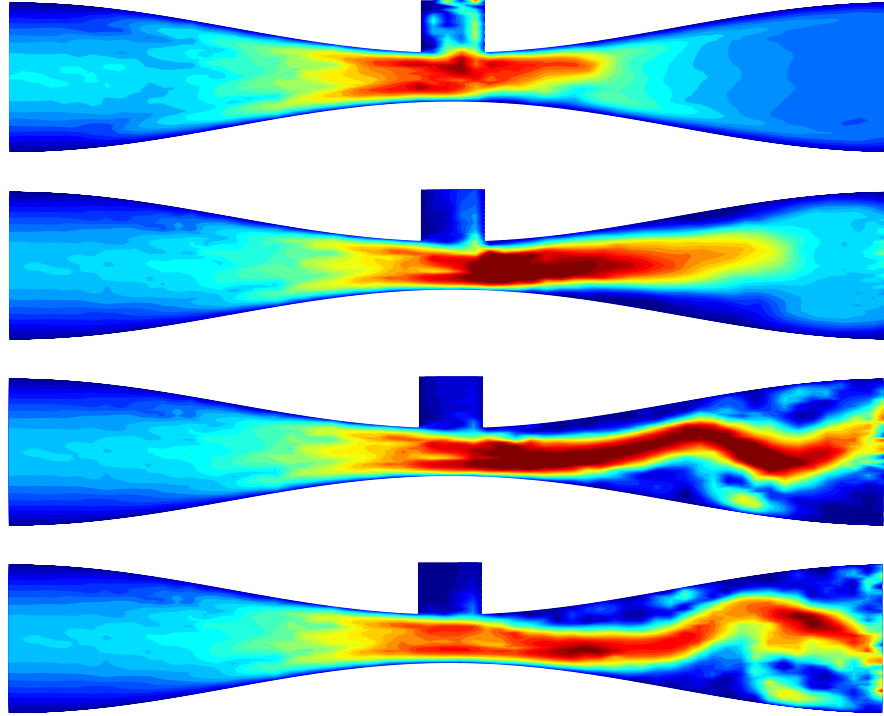


Figure 4: Shown above is the coarse mesh NSE ('no model') solution at $T=1,2,3,4$, from top to bottom, displayed as speed contours. Oscillations are present, and the flow pattern does not match that of the fine mesh solution, particularly at $T=4$ on the right hand side of the contraction.

4 A finite element algorithm for MHD-Voigt

We now consider a finite element discretization of the Voigt regularization of evolution equations for incompressible MHD flow. We will present a numerical scheme, analyze its stability and convergence, and then use it to approximate solutions to two benchmark test problems. To the best of our knowledge, the proposed scheme is new, and the analysis of it is the first numerical analysis performed for a discrete MHD-Voigt algorithm.

The following system of conservation laws governs the behavior of conducting, non-magnetic fluids, such as salt water, liquid metals, plasmas and strong electrolytes [7]. It was first developed by Ladyzhenskaya, and has since been studied in, e.g., [11, 12, 13, 23, 24].

$$u_t + \nabla \cdot (uu^T) - Re^{-1}\Delta u + \frac{s}{2}\nabla(B \cdot B) - s\nabla \cdot BB^T + \nabla p = f, \quad (4.1a)$$

$$\nabla \cdot u = 0, \quad (4.1b)$$

$$B_t + Re_m^{-1}\nabla \times (\nabla \times B) + \nabla \times (B \times u) = \nabla \times g, \quad (4.1c)$$

$$\nabla \cdot B = 0. \quad (4.1d)$$

Here, u is velocity, p is pressure, f is body force, $\nabla \times g$ is a forcing on the magnetic field B , Re is the Reynolds number, Re_m is the magnetic Reynolds number, and s is the coupling number.

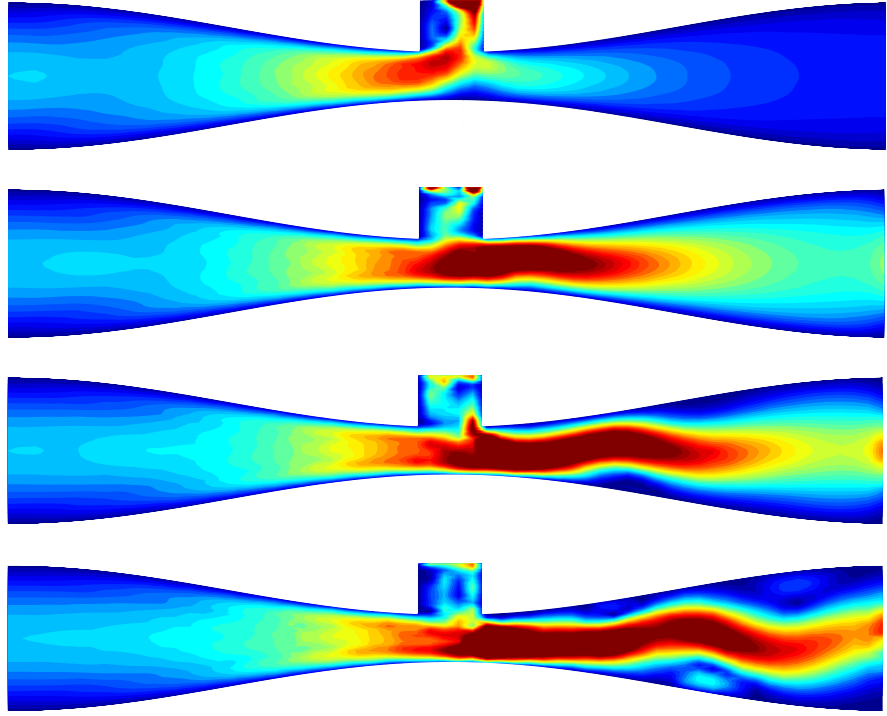


Figure 5: Shown above is the coarse mesh NSE-Voigt solution at $T=1,2,3,4$, from top to bottom, displayed as speed contours. There appears to be only minor oscillations, and the overall flow pattern matches that of the fine mesh NSE solution very well.

The MHD-Voigt system was first proposed and studied in [17], and is derived from (4.1a)-(4.1d) by adding a regularization term to each of the momentum and magnetic field equations, and takes the form

$$u_t + \nabla \cdot (uu^T) - Re^{-1}\Delta u + \frac{s}{2}\nabla(B \cdot B) - s\nabla \cdot BB^T + \nabla p - \alpha_1^2\Delta u_t = f, \quad (4.2a)$$

$$\nabla \cdot u = 0, \quad (4.2b)$$

$$B_t + Re_m^{-1}\nabla \times (\nabla \times B) + \nabla \times (B \times u) - \alpha_2^2\Delta B_t = \nabla \times g, \quad (4.2c)$$

$$\nabla \cdot B = 0. \quad (4.2d)$$

We now proceed to derive a numerical scheme to approximate solutions to (4.2a)-(4.2d), analyze its stability and convergence properties to solutions of (4.1a)-(4.1d), and test it on benchmark problems.

We begin the derivation by expanding the curl operator in the (4.2c) equation, and using that $\nabla \cdot u = \nabla \cdot B = 0$ to get

$$u_t - Re^{-1}\Delta u + u \cdot \nabla u + \frac{s}{2}\nabla(B \cdot B) - sB \cdot \nabla B + \nabla p - \alpha_1^2\Delta u_t = f, \quad (4.3a)$$

$$\nabla \cdot u = 0, \quad (4.3b)$$

$$B_t + Re_m^{-1}\nabla \times (\nabla \times B) + u \cdot \nabla B - B \cdot \nabla u - \alpha_2^2\Delta B_t = \nabla \times g, \quad (4.3c)$$

$$\nabla \cdot B = 0. \quad (4.3d)$$

Denote by $P := p + \frac{s}{2}|B|^2$ a modified pressure, use a vector identity for the Laplacian, and define $\lambda := Re_m \nabla \cdot B (= 0)$, which will act as a Lagrange multiplier corresponding to the

solenoidal constraint of the magnetic field. When using mixed finite element methods to discretize the system, using the discrete dummy variable λ in this way will allow for an explicit enforcement of a divergence free magnetic field. We now have the system

$$u_t - Re^{-1} \Delta u + u \cdot \nabla u - sB \cdot \nabla B + \nabla P - \alpha_1^2 \Delta u_t = f, \quad (4.4a)$$

$$\nabla \cdot u = 0, \quad (4.4b)$$

$$B_t - Re_m^{-1} \Delta B + u \cdot \nabla B - B \cdot \nabla u - \nabla \lambda - \alpha_2^2 \Delta B_t = \nabla \times g, \quad (4.4c)$$

$$\nabla \cdot B = 0. \quad (4.4d)$$

The numerical scheme is now derived with a Galerkin finite element spatial discretization and (four leg) trapezoidal time discretization. For simplicity, we require the discrete initial conditions be point-wise divergence free, that is, $u_h^0 = u_0$ and $B_h^0 = B_0$ must be in V_h . The resulting discrete problem now reads: For all $(v_h, \chi_h, q_h, r_h) \in (X_h, X_h, Q_h, Q_h)$, find $(u_h^{n+1}, B_h^{n+1}, P_h^{n+\frac{1}{2}}, \lambda_h^{n+\frac{1}{2}}) \in (X_h, X_h, Q_h, Q_h)$ for $n = 0, 1, 2, \dots, M = \frac{T}{\Delta t}$,

$$\begin{aligned} & \frac{1}{\Delta t} (u_h^{n+1} - u_h^n, v_h) + \frac{\alpha_1^2}{\Delta t} (\nabla(u_h^{n+1} - u_h^n), \nabla v_h) + (u_h^{n+\frac{1}{2}} \cdot \nabla u_h^{n+\frac{1}{2}}, v_h) \\ & + Re^{-1} (\nabla u_h^{n+\frac{1}{2}}, \nabla v_h) - s(B_h^{n+\frac{1}{2}} \cdot \nabla B_h^{n+\frac{1}{2}}, v_h) - (P_h^{n+\frac{1}{2}}, \nabla \cdot v_h) = (f(t^{n+\frac{1}{2}}), v_h), \end{aligned} \quad (4.5a)$$

$$(\nabla \cdot u_h^{n+1}, q_h) = 0, \quad (4.5b)$$

$$\begin{aligned} & \frac{1}{\Delta t} (B_h^{n+1} - B_h^n, \chi_h) + \frac{\alpha_2^2}{\Delta t} (\nabla(B_h^{n+1} - B_h^n), \nabla \chi_h) + Re_m^{-1} (\nabla B_h^{n+\frac{1}{2}}, \nabla \chi_h) \\ & - (B_h^{n+\frac{1}{2}} \cdot \nabla u_h^{n+\frac{1}{2}}, \chi_h) + (u_h^{n+\frac{1}{2}} \cdot \nabla B_h^{n+\frac{1}{2}}, \chi_h) + (\lambda_h^{n+\frac{1}{2}}, \nabla \cdot \chi_h) = (\nabla \times g(t^{n+\frac{1}{2}}), \chi_h), \end{aligned} \quad (4.5c)$$

$$(\nabla \cdot B_h^{n+1}, r_h) = 0. \quad (4.5d)$$

Remark 4.1. A linearization of (4.5a)-(4.5d) can be derived by using linear extrapolation in the first component each of the 4 nonlinear terms via the substitution

$$(u_h^{n+1/2} \cdot \nabla u_h^{n+1/2}, v_h) \rightarrow \left(\left(\frac{3}{2} u_h^n - \frac{1}{2} u_h^{n-1} \right) \cdot \nabla u_h^{n+1/2}, v_h \right),$$

and defining $u_h^{-1} := u_h^0$ (and similarly for the other nonlinear terms). The unconditional stability and convergence results that follow can be adapted to this linearized scheme with some minor, although technical, changes.

Remark 4.2. We analyze the scheme for the case of homogeneous Dirichlet boundary conditions for both the velocity and magnetic field. The exact analysis holds for the periodic case, and extension to inhomogeneous Dirichlet boundaries can be done in the usual way. The numerical tests we present herein use these two types of boundary conditions.

However, we note that if restricted to a convex domain, it is sufficient to enforce only $B \cdot n = 0$, where n is the outward unit normal vector, along with the natural boundary condition $(\nabla \times B) \times n = 0$. The scheme (4.5a)-(4.5d) and the analysis that follows can be adjusted to handle these boundary conditions with relatively minor changes.

4.1 Numerical analysis of the FE scheme for MHD-Voigt

We prove here that the scheme is both unconditionally stable with respect to time step, and optimally convergent. We begin with stability.

Lemma 4.1. *Solutions to the scheme (4.5a)-(4.5d) are stable for any $\Delta t > 0$, provided $u_0 \in H^1(\Omega)$, $B_0 \in H^1(\Omega)$, $f \in L^2(0, T; H^{-1}(\Omega))$ and $g \in L^2(0, T; L^2(\Omega))$, and satisfy*

$$\begin{aligned} & \|u_h^M\|^2 + s \|B_h^M\|^2 + \alpha_1^2 \|\nabla u_h^M\| + s \alpha_2^2 \|\nabla B_h^M\| + \Delta t \sum_{n=0}^{M-1} \left(Re^{-1} \left\| \nabla u_h^{n+\frac{1}{2}} \right\|^2 + s Re_m^{-1} \left\| \nabla B_h^{n+\frac{1}{2}} \right\|^2 \right) \\ & \leq \|u_h^0\|^2 + s \|B_h^0\|^2 + \alpha_1^2 \|\nabla u_h^0\|^2 + s \alpha_2^2 \|\nabla B_h^0\|^2 + \Delta t \sum_{n=0}^{M-1} \left(Re \left\| f(t^{n+\frac{1}{2}}) \right\|_{-1}^2 + s Re_m \left\| g(t^{n+\frac{1}{2}}) \right\|^2 \right) \\ & = C(Re, Re_m, f, g, u_0, B_0, s). \quad (4.6) \end{aligned}$$

Proof. We begin this proof by setting $v_h = u_h^{n+1/2}$ and $\chi_h = B_h^{n+1/2}$ in (4.5a) and (4.5c) (which are guaranteed to be in V_h due to (4.5b) and (4.5d)), respectively, then adding the equations, multiplying through by Δt and summing from $n = 0$ to $M - 1$. This gives

$$\begin{aligned} & \left(\frac{1}{2} \left(\|u_h^M\|^2 + \alpha_1^2 \|\nabla u_h^M\| \right) + \frac{s}{2} \left(\|B_h^M\|^2 + \alpha_2^2 \|\nabla B_h^M\|^2 \right) \right) \\ & + \Delta t \sum_{n=0}^{M-1} \left(Re^{-1} \left\| \nabla u_h^{n+\frac{1}{2}} \right\|^2 + s Re_m^{-1} \left\| \nabla B_h^{n+\frac{1}{2}} \right\|^2 \right) \\ & = \left(\frac{1}{2} \left(\|u_h^0\|^2 + \alpha_1^2 \|\nabla u_h^0\| \right) + \frac{s}{2} \left(\|B_h^0\|^2 + \alpha_2^2 \|\nabla B_h^0\|^2 \right) \right) \\ & + \Delta t \sum_{n=0}^{M-1} \left((f(t^{n+\frac{1}{2}}), u_h^{n+\frac{1}{2}}) + s(\nabla \times g(t^{n+\frac{1}{2}}), B_h^{n+\frac{1}{2}}) \right) \quad (4.7) \end{aligned}$$

The forcing terms can be majorized with Cauchy-Schwarz and Young's inequalities to get

$$(f(t^{n+\frac{1}{2}}), u_h^{n+\frac{1}{2}}) \leq \frac{Re}{2} \left\| f(t^{n+\frac{1}{2}}) \right\|_{-1}^2 + \frac{Re^{-1}}{2} \left\| \nabla u_h^{n+1/2} \right\|^2, \quad (4.8)$$

$$s(\nabla \times g(t^{n+\frac{1}{2}}), B_h^{n+\frac{1}{2}}) \leq \frac{s Re_m}{2} \left\| g(t^{n+\frac{1}{2}}) \right\|^2 + \frac{s Re_m^{-1}}{2} \left\| \nabla B_h^{n+\frac{1}{2}} \right\|^2. \quad (4.9)$$

Using (4.8) and (4.9) in (4.7) proves the lemma. \square

We now prove convergence of the scheme.

Theorem 4.1. *Assume (u, p, B) solves (4.1a)-(4.1d) and satisfies the following regularity: $B_t, u_t \in L^\infty(0, T; H^1(\Omega))$, $B_{tt}, u_{tt}, \nabla B_{tt}, \nabla u_{tt} \in L^2(0, T, L^2(\Omega))$, $B_{ttt}, u_{ttt} \in L^2(0, T; L^2(\Omega))$, and $B, u \in L^\infty(0, T; H^m(\Omega))$, where $m = \max(3, k)$. Then for Δt small enough, the solution $(u_h, p_h, B_h, \lambda_h)$ to (4.5a)-(4.5d) converges to the true solution with rate*

$$\left(\Delta t \sum_{n=0}^{M-1} \left(\left\| \nabla u(t^{n+1/2}) - \nabla u_h^{n+1/2} \right\|^2 + \left\| \nabla B(t^{n+1/2}) - \nabla B_h^{n+1/2} \right\|^2 \right) \right)^{1/2} = O(\Delta t^2 + h^k + \alpha_1^2 + \alpha_2^2).$$

Remark 4.3. *The convergence theorem shows that α_1, α_2 should be chosen to satisfy*

$$\alpha_1, \alpha_2 \leq C \max \{ \Delta t, h^{k/2} \}$$

in order for the scheme to achieve optimal convergence.

Proof. Throughout this proof, the constant C can depend on problem data and the true solution, and can change its value at any step of the proof, but is independent of h , Δt , α_1 , α_2 .

Multiply the momentum and magnetic field equations (4.1a), (4.1c) at $t^{n+1/2}$ by $v_h \in V_h$ and $\chi_h \in V_h$, respectively, and integrate over the domain. Next, add $\frac{\alpha_1^2}{\Delta t}(\nabla u(t^{n+1}) - \nabla u(t^n), \nabla v_h)$ to both sides of the momentum equation, and $\frac{\alpha_2^2}{\Delta t}(\nabla B(t^{n+1}) - \nabla B(t^n), \nabla \chi_h)$ to both sides of the magnetic field equation. Denoting $e_u^k = u_h^k - u^k$, $e_B^k = B_h^k - B^k$, we get

$$\begin{aligned} & (u_t(t^{n+1/2}), v_h) + (u(t^{n+1/2}) \cdot \nabla u(t^{n+1/2}), v_h) + Re^{-1}(\nabla u(t^{n+1/2}), \nabla v_h) - s(B(t^{n+1/2}) \cdot \nabla B(t^{n+1/2}), v_h) \\ & \quad + \alpha_1^2(\nabla u_t(t^{n+1/2}), \nabla v_h) + \frac{\alpha_1^2}{\Delta t}(\nabla u(t^{n+1}) - \nabla u(t^n), \nabla v_h) \\ & \quad = (f(t^{n+1/2}), v_h)) + \frac{\alpha_1^2}{\Delta t}(\nabla u(t^{n+1}) - \nabla u(t^n), \nabla v_h) \end{aligned} \quad (4.10)$$

$$\begin{aligned} & (B_t(t^{n+1/2}), \chi_h) + Re_m^{-1}(\nabla B(t^{n+1/2}), \nabla \chi_h) - (B(t^{n+1/2}) \cdot \nabla u(t^{n+1/2}), \chi_h) \\ & \quad + (u(t^{n+1/2}) \cdot \nabla B(t^{n+1/2}), \chi_h) + \alpha_2^2 \nabla(B_t(t^{n+1/2}), \nabla \chi_h) + \frac{\alpha_2^2}{\Delta t}(\nabla B(t^{n+1}) - \nabla B(t^n), \nabla \chi_h) \\ & \quad = (\nabla \times g(t^{n+1/2}), \chi_h) + \frac{\alpha_2^2}{\Delta t}(\nabla B(t^{n+1}) - \nabla B(t^n), \nabla \chi_h). \end{aligned} \quad (4.11)$$

As usual, we will look to subtract the continuous formulation of the variational problem from the discrete formulation. We start this process by introducing the following terms (4.12)-(4.15), which replace the terms in the left-hand side of (4.10). To simplify notation, we use \pm to denote adding and subtracting the same term.

$$\begin{aligned} & (u_t(t^{n+1/2}), v_h) \pm \frac{1}{\Delta t}(u(t^{n+1}) - u(t^n), v_h) = \frac{1}{\Delta t}(u(t^{n+1}) - u(t^n), v_h) \\ & \quad + (u_t(t^{n+1/2}) - \{u(t^{n+1}) - u(t^n)\} \Delta t^{-1}, v_h). \end{aligned} \quad (4.12)$$

$$\begin{aligned} & (u(t^{n+1/2}) \cdot \nabla u(t^{n+1/2}), v_h) \pm (u^{n+1/2} \cdot \nabla u^{n+1/2}, v_h) = (u(t^{n+1/2}) \cdot \nabla(u(t^{n+1/2}) - u^{n+1/2}), v_h) \\ & \quad + ((u(t^{n+1/2}) - u^{n+1/2}) \cdot \nabla u^{n+1/2}, v_h) + (u^{n+1/2} \cdot \nabla u^{n+1/2}, v_h). \end{aligned} \quad (4.13)$$

$$\begin{aligned} & Re^{-1} \left((\nabla u(t^{n+1/2}), \nabla v_h) \pm (\nabla u^{n+1/2}, \nabla v_h) \right) \\ & \quad = Re^{-1}(\nabla(u(t^{n+1/2}) - u^{n+1/2}), \nabla v_h) + Re^{-1}(\nabla u^{n+1/2}, \nabla v_h) \end{aligned} \quad (4.14)$$

$$\begin{aligned} & -s(B(t^{n+1/2}) \cdot \nabla B(t^{n+1/2}), v_h) \pm s(B^{n+1/2} \cdot \nabla B^{n+1/2}, v_h) = s(B^{n+1/2} \cdot \nabla(B^{n+1/2} - B(t^{n+1/2})), v_h) \\ & \quad + s((B^{n+1/2} - B(t^{n+1/2})) \cdot \nabla B(t^{n+1/2}), v_h) - s(B^{n+1/2} \cdot \nabla B^{n+1/2}, v_h). \end{aligned} \quad (4.15)$$

$$\begin{aligned} & \alpha_1^2(\nabla u_t(t^{n+1/2}), \nabla v_h) \pm \frac{\alpha_1^2}{\Delta t}(\nabla(u(t^{n+1}) - u(t^n)), \nabla v_h) = \frac{\alpha_1^2}{\Delta t}(\nabla(u(t^{n+1}) - u(t^n)), \nabla v_h) \\ & \quad + \alpha_1^2(\nabla(u_t(t^{n+1/2}) - \{u(t^{n+1}) - u(t^n)\} \Delta t^{-1}), \nabla v_h). \end{aligned} \quad (4.16)$$

Now we can directly subtract (4.10) from (4.5a),

$$\begin{aligned}
& \frac{1}{\Delta t} (e_u^{n+1} - e_u^n, v_h) + Re^{-1} (\nabla e_u^{n+\frac{1}{2}}, \nabla v_h) + (u_h^{n+\frac{1}{2}} \cdot \nabla e_u^{n+\frac{1}{2}}, v_h) + (e_u^{n+\frac{1}{2}} \cdot \nabla u^{n+\frac{1}{2}}, v_h) \\
& \quad - s(B_h^{n+\frac{1}{2}} \cdot \nabla e_B^{n+\frac{1}{2}}, v_h) - s(e_B^{n+\frac{1}{2}} \cdot \nabla B^{n+\frac{1}{2}}, v_h) + \frac{\alpha_1^2}{\Delta t} (\nabla(e_u^{n+1} - e_u^n), \nabla v_h) \\
& = (u_t(t^{n+\frac{1}{2}}) - \{u(t^{n+1}) - u(t^n)\} \Delta t^{-1}, v_h) + Re^{-1} (\nabla(u(t^{n+\frac{1}{2}}) - u^{n+\frac{1}{2}}), \nabla v_h) \\
& \quad + (u(t^{n+\frac{1}{2}}) \cdot \nabla(u(t^{n+\frac{1}{2}}) - u^{n+\frac{1}{2}}), v_h) + ((u(t^{n+\frac{1}{2}}) - u^{n+\frac{1}{2}}) \cdot \nabla u^{n+\frac{1}{2}}, v_h) \\
& \quad + s((B^{n+\frac{1}{2}} - B(t^{n+\frac{1}{2}})) \cdot \nabla B(t^{n+\frac{1}{2}}), v_h) + s(B^{n+\frac{1}{2}} \cdot \nabla(B^{n+\frac{1}{2}} - B(t^{n+\frac{1}{2}})), v_h) \\
& \quad + \alpha_1^2 (\nabla u_t(t^{n+\frac{1}{2}}), \nabla v_h) - \alpha_1^2 (\nabla(u_t(t^{n+\frac{1}{2}}) - \{u(t^{n+1}) - u(t^n)\} \Delta t^{-1}), \nabla v_h) =: G_1(t, B, u, v_h)
\end{aligned} \tag{4.17}$$

Note that G_1 represents terms associated only with the true solution. Using the assumptions on the regularity of the solution, standard analysis (Taylor series, Cauchy-Schwarz and Young's inequalities, see e.g. [20]) provides

$$\begin{aligned}
|G_1(t, B, u, v_h)| &\leq C(\Delta t^2 \|v_h\| + \alpha_1^2(\Delta t^2 + 1) \|\nabla v_h\|) \\
&\leq C\Delta t^4 + C\|v_h\|^2 + \frac{Re^{-1}}{8} \|\nabla v_h\|^2 + C\alpha_1^4 \Delta t^4 + C\alpha_1^4.
\end{aligned} \tag{4.18}$$

Similarly for the magnetic field equation, we have

$$\begin{aligned}
& \frac{1}{\Delta t} (e_B^{n+1} - e_B^n, \chi_h) + Re_m^{-1} (\nabla e_B^{n+\frac{1}{2}}, \nabla \chi_h) - (B_h^{n+\frac{1}{2}} \cdot \nabla e_u^{n+\frac{1}{2}}, \chi_h) - (e_B^{n+\frac{1}{2}} \cdot \nabla u^{n+\frac{1}{2}}, \chi_h) \\
& \quad + (u^{n+\frac{1}{2}} \cdot \nabla e_B^{n+\frac{1}{2}}, \chi_h) + (e_u^{n+\frac{1}{2}} \cdot \nabla B^{n+\frac{1}{2}}, \chi_h) + \frac{\alpha_2^2}{\Delta t} (\nabla(e_B^{n+1} - e_B^n), \nabla \chi_h) \\
& = (B_t(t^{n+\frac{1}{2}}) - \{B(t^{n+1}) - B(t^n)\} \Delta t^{-1}, \chi_h) \\
& \quad + Re_m^{-1} (\nabla(B(t^{n+\frac{1}{2}}) - B^{n+\frac{1}{2}}), \nabla \chi_h) \\
& \quad + (B(t^{n+\frac{1}{2}}) \cdot \nabla(u^{n+\frac{1}{2}} - u(t^{n+\frac{1}{2}})), \chi_h) + ((B^{n+\frac{1}{2}} - B(t^{n+\frac{1}{2}})) \cdot \nabla u^{n+\frac{1}{2}}, \chi_h) \\
& \quad + (u(t^{n+\frac{1}{2}}) \cdot \nabla(B(t^{n+\frac{1}{2}}) - B^{n+\frac{1}{2}}), \chi_h) + ((u(t^{n+\frac{1}{2}}) - u^{n+\frac{1}{2}}) \cdot \nabla B^{n+\frac{1}{2}}, \chi_h) \\
& \quad + \alpha_2^2 (\nabla B_t(t^{n+\frac{1}{2}}), \nabla \chi_h) - \alpha_2^2 (\nabla(B_t(t^{n+\frac{1}{2}}) - \{B(t^{n+1}) - B(t^n)\} \Delta t^{-1}), \nabla \chi_h) \\
& =: G_2(t, B, u, \chi_h)
\end{aligned} \tag{4.19}$$

Similar to G_1 , we bound G_2 by

$$\begin{aligned}
|G_2(t, B, u, \chi_h)| &\leq C(\Delta t^2 \|\chi_h\| + \alpha_2^2(\Delta t^2 + 1) \|\nabla \chi_h\|) \\
&\leq C\Delta t^4 + C\|\chi_h\|^2 + \frac{Re^{-1}}{8} \|\nabla \chi_h\|^2 + C\alpha_2^4 \Delta t^4 + C\alpha_2^4.
\end{aligned} \tag{4.20}$$

Define $\phi_h^n = (u_h^n - U^n)$ and $\eta^n = (u^n - U^n) \Rightarrow e_u^n = \phi_h^n - \eta_u^n$ and analogously $e_B^n = (B_h^n - \mathcal{B}^n) + (\mathcal{B}^n - B^n) = \psi_h^n - \eta_B^n$, where $U^k \in V_h$ and $\mathcal{B}^k \in V_h$. Substituting into (4.17) and (4.19) results in:

$$\begin{aligned}
& \frac{1}{\Delta t}(\phi_h^{n+1} - \phi_h^n, v_h) + Re^{-1}(\nabla \phi_h^{n+\frac{1}{2}}, \nabla v_h) + (u_h^{n+\frac{1}{2}} \cdot \nabla \phi_h^{n+\frac{1}{2}}, v_h) + (\phi_h^{n+\frac{1}{2}} \cdot \nabla u^{n+\frac{1}{2}}, v_h) \\
& \quad - s(B_h^{n+\frac{1}{2}} \cdot \nabla \psi_h^{n+\frac{1}{2}}, v_h) - s(\psi_h^{n+\frac{1}{2}} \cdot \nabla B^{n+\frac{1}{2}}, v_h) + \frac{\alpha_1^2}{\Delta t}(\nabla(\phi_h^{n+1} - \phi_h^n), \nabla v_h) \\
= & \frac{1}{\Delta t}(\eta_u^{n+1} - \eta_u^n, v_h) + Re^{-1}(\nabla \eta_u^{n+\frac{1}{2}}, \nabla v_h) + (u_h^{n+\frac{1}{2}} \cdot \nabla \eta_u^{n+\frac{1}{2}}, v_h) \\
& \quad + (\eta_u^{n+\frac{1}{2}} \cdot \nabla u^{n+\frac{1}{2}}, v_h) - s(B_h^{n+\frac{1}{2}} \cdot \nabla \eta_B^{n+\frac{1}{2}}, v_h) \\
& \quad - s(\eta_B^{n+\frac{1}{2}} \cdot \nabla B^{n+\frac{1}{2}}, v_h) + \frac{\alpha_1^2}{\Delta t}(\nabla(\eta_u^{n+1} - \eta_u^n), \nabla v_h) + G_1(t, u, B, v_h)
\end{aligned} \tag{4.21}$$

$$\begin{aligned}
& \frac{1}{\Delta t}(\psi_h^{n+1} - \psi_h^n, \chi_h) + Re_m^{-1}(\nabla \psi_h^{n+1}, \nabla \chi_h) - (B_h^{n+\frac{1}{2}} \cdot \nabla \phi_h^{n+\frac{1}{2}}, \chi_h) - (\psi_h^{n+\frac{1}{2}} \cdot \nabla u^{n+\frac{1}{2}}, \chi_h) \\
& \quad + (u^{n+\frac{1}{2}} \cdot \nabla \psi_h^{n+\frac{1}{2}}, \chi_h) + (\phi_h^{n+\frac{1}{2}} \cdot \nabla B^{n+\frac{1}{2}}, \chi_h) + \frac{\alpha_2^2}{\Delta t}(\nabla(\psi_h^{n+1} - \psi_h^n), \nabla \chi_h) \\
= & \frac{1}{\Delta t}(\eta_B^{n+1} - \eta_B^n, \chi_h) + Re_m^{-1}(\nabla \eta_B^{n+\frac{1}{2}}, \nabla \chi_h) - (B_h^{n+\frac{1}{2}} \cdot \nabla \eta_u^{n+\frac{1}{2}}, \chi_h) \\
& \quad - (\eta_B^{n+\frac{1}{2}} \cdot \nabla u^{n+\frac{1}{2}}, \chi_h) + (u^{n+\frac{1}{2}} \cdot \nabla \eta_B^{n+\frac{1}{2}}, \chi_h) + (\eta_u^{n+\frac{1}{2}} \cdot \nabla B^{n+\frac{1}{2}}, \chi_h) \\
& \quad + \frac{\alpha_2^2}{\Delta t}(\nabla(\eta_b^{n+1} - \eta_b^n), \nabla \chi_h) + G_2(t, u, B, \chi_h)
\end{aligned} \tag{4.22}$$

Taking $\chi_h = \psi_h^{n+\frac{1}{2}}$ and $v_h = \phi_h^{n+\frac{1}{2}}$ in (4.21) and (4.22), then simplifying yields the equations

$$\begin{aligned}
& \frac{1}{2\Delta t}(\|\phi_h^{n+1}\|^2 - \|\phi_h^n\|^2) + Re^{-1}\left\|\nabla \phi_h^{n+\frac{1}{2}}\right\|^2 + (\phi_h^{n+\frac{1}{2}} \cdot \nabla u^{n+\frac{1}{2}}, \phi_h^{n+\frac{1}{2}}) - s(B_h^{n+\frac{1}{2}} \cdot \nabla \psi_h^{n+\frac{1}{2}}, \phi_h^{n+\frac{1}{2}}) \\
& \quad - s(\psi_h^{n+\frac{1}{2}} \cdot \nabla B^{n+\frac{1}{2}}, \phi_h^{n+\frac{1}{2}}) + \frac{\alpha_1^2}{2\Delta t}(\|\nabla \phi_h^{n+1}\|^2 - \|\nabla \phi_h^n\|^2) \\
= & \frac{1}{\Delta t}(\eta_u^{n+1} - \eta_u^n, \phi_h^{n+\frac{1}{2}}) + Re^{-1}(\nabla \eta_u^{n+\frac{1}{2}}, \nabla \phi_h^{n+\frac{1}{2}}) + (u_h^{n+\frac{1}{2}} \cdot \nabla \eta_u^{n+\frac{1}{2}}, \phi_h^{n+\frac{1}{2}}) \\
& \quad + (\eta_u^{n+\frac{1}{2}} \cdot \nabla u^{n+\frac{1}{2}}, \phi_h^{n+\frac{1}{2}}) - s(B_h^{n+\frac{1}{2}} \cdot \nabla \eta_B^{n+\frac{1}{2}}, \phi_h^{n+\frac{1}{2}}) - s(\eta_B^{n+\frac{1}{2}} \cdot \nabla B^{n+\frac{1}{2}}, \phi_h^{n+\frac{1}{2}}) \\
& \quad + \frac{\alpha_1^2}{\Delta t}(\nabla \eta_u^{n+1} - \nabla \eta_u^n, \nabla \phi_h^{n+\frac{1}{2}}) + G_1(t, u, B, \phi_h^{n+\frac{1}{2}})
\end{aligned} \tag{4.23}$$

and

$$\begin{aligned}
& \frac{1}{2\Delta t} \left(\left\| \psi_h^{n+\frac{1}{2}} \right\|^2 - \left\| \psi_h^{n+\frac{1}{2}} \right\|^2 \right) + Re_m^{-1} \left\| \nabla \psi_h^{n+\frac{1}{2}} \right\|^2 - (B_h^{n+\frac{1}{2}} \cdot \nabla \phi_h^{n+\frac{1}{2}}, \psi_h^{n+\frac{1}{2}}) - (\psi_h^{n+\frac{1}{2}} \cdot \nabla u^{n+\frac{1}{2}}, \psi_h^{n+\frac{1}{2}}) \\
& + (\phi_h^{n+\frac{1}{2}} \cdot \nabla B^{n+\frac{1}{2}}, \psi_h^{n+\frac{1}{2}}) + \frac{\alpha_2^2}{2\Delta t} \left(\left\| \nabla \psi_h^{n+\frac{1}{2}} \right\|^2 - \left\| \nabla \psi_h^{n+\frac{1}{2}} \right\|^2 \right) \\
& = \frac{1}{\Delta t} (\eta_B^{n+1} - \eta_B^n, \psi_h^{n+\frac{1}{2}}) + Re_m^{-1} (\nabla \eta_B^{n+\frac{1}{2}}, \nabla \psi_h^{n+\frac{1}{2}}) - (B_h^{n+\frac{1}{2}} \cdot \nabla \eta_u^{n+\frac{1}{2}}, \psi_h^{n+\frac{1}{2}}) \\
& - (\eta_B^{n+\frac{1}{2}} \cdot \nabla u^{n+\frac{1}{2}}, \psi_h^{n+\frac{1}{2}}) + (u^{n+\frac{1}{2}} \cdot \nabla \eta_B^{n+\frac{1}{2}}, \psi_h^{n+\frac{1}{2}}) + (\eta_u^{n+\frac{1}{2}} \cdot \nabla B^{n+\frac{1}{2}}, \psi_h^{n+\frac{1}{2}}) \\
& + \frac{\alpha_2^2}{\Delta t} (\nabla \eta_B^{n+1} - \nabla \eta_B^n, \nabla \psi_h^{n+\frac{1}{2}}) + G_2(t, u, B, \psi_h^{n+\frac{1}{2}}) \quad (4.24)
\end{aligned}$$

Using the inequalities,

$$\frac{1}{\Delta t} (\eta_u^{n+1} - \eta_u^n, \phi_h^{n+\frac{1}{2}}) \leq \frac{1}{2\Delta t} \int_{t^n}^{t^{n+1}} \|\partial(\eta_u)\|^2 dt + \frac{1}{2} \left\| \phi_h^{n+\frac{1}{2}} \right\|^2, \quad (4.25)$$

$$\frac{\alpha_1^2}{\Delta t} (\nabla \eta_u^{n+1} - \nabla \eta_u^n, \nabla \phi_h^{n+\frac{1}{2}}) \leq \frac{\alpha_1^2}{2\Delta t} \int_{t^n}^{t^{n+1}} \|\partial(\nabla \eta_u)\|^2 dt + \frac{\alpha_1^2}{2} \left\| \nabla \phi_h^{n+\frac{1}{2}} \right\|^2, \quad (4.26)$$

along with Hölder's Inequality and (4.18),

$$\begin{aligned}
& \frac{1}{2\Delta t} (\|\phi_h^{n+1}\|^2 - \|\phi_h^n\|^2) + \frac{Re^{-1}}{2} \left\| \nabla \phi_h^{n+\frac{1}{2}} \right\|^2 + \frac{\alpha_1^2}{2\Delta t} (\|\nabla \phi_h^{n+1}\|^2 - \|\nabla \phi_h^n\|^2) \\
& \leq \frac{1}{2\Delta t} \int_{t^n}^{t^{n+1}} (\|\partial_t(\eta_u)\|^2 + \alpha_1^2 \|\nabla \partial_t(\eta_u)\|^2) dt + \frac{1}{2} \left\| \phi_h^{n+\frac{1}{2}} \right\|^2 + \frac{\alpha_1^2}{2} \left\| \nabla \phi_h^{n+\frac{1}{2}} \right\|^2 + \left(\frac{Re^{-1}}{2} \right) \left\| \nabla \eta_u^{n+\frac{1}{2}} \right\|^2 \\
& + \left\| \nabla u^{n+\frac{1}{2}} \right\|_\infty \left\| \phi_h^{n+\frac{1}{2}} \right\|^2 + s (B_h^{n+\frac{1}{2}} \cdot \nabla \psi_h^{n+\frac{1}{2}}, \phi_h^{n+\frac{1}{2}}) + s \left\| \nabla B^{n+\frac{1}{2}} \right\|_\infty \left\| \psi_h^{n+\frac{1}{2}} \right\| \left\| \phi_h^{n+\frac{1}{2}} \right\| \\
& + C \left\| \nabla u_h^{n+\frac{1}{2}} \right\| \left\| \nabla \eta_u^{n+\frac{1}{2}} \right\| \left\| \nabla \phi_h^{n+\frac{1}{2}} \right\| + \left\| \nabla u^{n+\frac{1}{2}} \right\|_\infty \left\| \eta_u^{n+\frac{1}{2}} \right\| \left\| \phi_h^{n+\frac{1}{2}} \right\| + Cs \left\| \nabla B_h^{n+\frac{1}{2}} \right\| \left\| \nabla \eta_B^{n+\frac{1}{2}} \right\| \left\| \nabla \phi_h^{n+\frac{1}{2}} \right\| \\
& + s \left\| \nabla B^{n+\frac{1}{2}} \right\|_\infty \left\| \eta_B^{n+\frac{1}{2}} \right\| \left\| \phi_h^{n+\frac{1}{2}} \right\| + C (\Delta t^4 + \|\phi^{n+\frac{1}{2}}\|^2 + \alpha_1^4 + \alpha_1^4 \Delta t^4) + \frac{Re^{-1}}{8} \|\nabla \phi_h^{n+\frac{1}{2}}\|^2 \\
& \quad (4.27)
\end{aligned}$$

This reduces, with Cauchy-Schwarz and Young's inequalities and the assumption of the regularity of the solution, to

$$\begin{aligned}
& \frac{1}{2\Delta t} (\|\phi_h^{n+1}\|^2 - \|\phi_h^n\|^2) + \frac{Re^{-1}}{8} \left\| \nabla \phi_h^{n+\frac{1}{2}} \right\|^2 + \frac{\alpha_1^2}{2\Delta t} (\|\nabla \phi_h^{n+1}\|^2 - \|\nabla \phi_h^n\|^2) \\
& \leq \frac{1}{2\Delta t} \int_{t^n}^{t^{n+1}} (\|\partial_t(\eta_u)\|^2 + \alpha_1^2 \|\nabla \partial_t(\eta_u)\|^2) dt + \frac{\alpha_1^2}{2} \left\| \nabla \phi_h^{n+\frac{1}{2}} \right\|^2 + \left(\frac{Re^{-1}}{2} \right) \left\| \nabla \eta_u^{n+\frac{1}{2}} \right\|^2 \\
& + C \left(\left\| \phi_h^{n+\frac{1}{2}} \right\|^2 + \left\| \psi_h^{n+\frac{1}{2}} \right\|^2 + \Delta t^4 + \alpha_1^4 + \alpha_1^4 \Delta t^4 + \left\| \eta_u^{n+\frac{1}{2}} \right\|^2 + \left\| \nabla u_h^{n+\frac{1}{2}} \right\|^2 \left\| \nabla \eta_u^{n+\frac{1}{2}} \right\|^2 \right. \\
& \quad \left. + s^2 \left\| \nabla B_h^{n+\frac{1}{2}} \right\|^2 \left\| \nabla \eta_B^{n+\frac{1}{2}} \right\|^2 + s^2 \left\| \eta_B^{n+\frac{1}{2}} \right\|^2 \right) + s (B_h^{n+\frac{1}{2}} \cdot \nabla \psi_h^{n+\frac{1}{2}}, \phi_h^{n+\frac{1}{2}}) \quad (4.28)
\end{aligned}$$

We now step back from (4.28) and return to (4.24), which can be majorized in a similar way as the momentum system, as

$$\begin{aligned}
& \frac{1}{2\Delta t} (\|\psi_h^{n+1}\|^2 - \|\psi_h^n\|^2) + \frac{Re_m^{-1}}{2} \|\nabla \psi_h^{n+1/2}\|^2 + \frac{\alpha_2^2}{2\Delta t} (\|\nabla \psi_h^{n+1}\|^2 - \|\nabla \psi_h^n\|^2) \\
& \leq \frac{1}{2\Delta t} \int_{t^n}^{t^{n+1}} (\|\partial_t(\eta_B)\|^2 + \alpha_2^2 \|\nabla \partial_t(\eta_B)\|^2) dt + \frac{1}{2} \left\| \psi_h^{n+\frac{1}{2}} \right\|^2 + \frac{\alpha_2^2}{2} \left\| \nabla \psi_h^{n+\frac{1}{2}} \right\|^2 + \frac{Re_m^{-1}}{2} \left\| \nabla \eta_B^{n+\frac{1}{2}} \right\|^2 \\
& \quad + (B_h^{n+\frac{1}{2}} \cdot \nabla \phi_h^{n+\frac{1}{2}}, \psi_h^{n+\frac{1}{2}}) + \left\| \nabla B_h^{n+\frac{1}{2}} \right\|_\infty \left\| \phi_h^{n+\frac{1}{2}} \right\| \left\| \psi_h^{n+\frac{1}{2}} \right\| + \left\| \nabla u^{n+\frac{1}{2}} \right\|_\infty \left\| \psi_h^{n+\frac{1}{2}} \right\|^2 \\
& \quad + C \left\| \nabla B_h^{n+\frac{1}{2}} \right\| \left\| \nabla \eta_u^{n+\frac{1}{2}} \right\| \left\| \nabla \psi_h^{n+\frac{1}{2}} \right\| + C \left\| \nabla u^{n+\frac{1}{2}} \right\|_\infty \left\| \nabla \eta_B^{n+\frac{1}{2}} \right\| \left\| \psi_h^{n+\frac{1}{2}} \right\| \\
& \quad + \left\| \nabla B_h^{n+\frac{1}{2}} \right\|_\infty \left\| \eta_u^{n+\frac{1}{2}} \right\| \left\| \psi_h^{n+\frac{1}{2}} \right\| + C \left(\Delta t^4 + \left\| \psi_h^{n+\frac{1}{2}} \right\|^2 + \alpha_2^4 + \alpha_2^4 \Delta t^4 \right) \quad (4.29)
\end{aligned}$$

Under the regularity assumptions, Cauchy-Schwarz and Young's inequalities, this can be reduced to

$$\begin{aligned}
& \frac{1}{2\Delta t} (\|\psi_h^{n+1}\|^2 - \|\psi_h^n\|^2) + \frac{Re_m^{-1}}{8} \|\nabla \psi_h^{n+1}\|^2 + \frac{\alpha_2^2}{2\Delta t} (\|\nabla \psi_h^{n+1}\|^2 - \|\nabla \psi_h^n\|^2) \\
& \leq \frac{1}{2\Delta t} \int_{t^n}^{t^{n+1}} (\|\partial_t(\eta_B)\|^2 + \alpha_2^2 \|\partial_t(\nabla \eta_B)\|^2) dt + \frac{\alpha_2^2}{2} \left\| \nabla \psi_h^{n+\frac{1}{2}} \right\|^2 \\
& + \frac{Re_m^{-1}}{2} \left\| \nabla \eta_B^{n+\frac{1}{2}} \right\|^2 + C \left(\left\| \psi_h^{n+\frac{1}{2}} \right\|^2 + \Delta t^4 + \Delta t^4 \alpha_2^2 + \alpha_2^4 + \left\| \phi_h^{n+\frac{1}{2}} \right\|^2 + \left\| \nabla \eta_B^{n+\frac{1}{2}} \right\|^2 + \left\| \eta_u^{n+\frac{1}{2}} \right\|^2 \right. \\
& \quad \left. + Re_m \left\| \nabla B_h^{n+\frac{1}{2}} \right\|^2 \left\| \nabla \eta_u^{n+\frac{1}{2}} \right\|^2 \right) + (B_h^{n+\frac{1}{2}} \cdot \nabla \phi_h^{n+\frac{1}{2}}, \psi_h^{n+\frac{1}{2}}). \quad (4.30)
\end{aligned}$$

Multiplying (4.30) by s and adding it to (4.28), and using that

$$(B_h^{n+\frac{1}{2}} \cdot \nabla \phi_h^{n+\frac{1}{2}}, \psi_h^{n+\frac{1}{2}}) = -(B_h^{n+\frac{1}{2}} \cdot \nabla \psi_h^{n+\frac{1}{2}}, \phi_h^{n+\frac{1}{2}}),$$

along with Poincare's inequality and reducing, we get

$$\begin{aligned}
& \frac{1}{2\Delta t} (\|\phi_h^{n+1}\|^2 - \|\phi_h^n\|^2) + \frac{s}{2\Delta t} (\|\psi_h^{n+1}\|^2 - \|\psi_h^n\|^2) + \frac{Re_m^{-1}}{8} \left\| \nabla \phi_h^{n+\frac{1}{2}} \right\|^2 + \frac{sRe_m^{-1}}{8} \left\| \nabla \psi_h^{n+\frac{1}{2}} \right\|^2 \\
& \quad + \frac{\alpha_1^2}{2\Delta t} (\|\nabla \phi_h^{n+1}\|^2 - \|\nabla \phi_h^n\|^2) + \frac{s\alpha_2^2}{2\Delta t} (\|\nabla \psi_h^{n+1}\|^2 - \|\nabla \psi_h^n\|^2) \\
& \leq \frac{1}{2\Delta t} \int_{t^n}^{t^{n+1}} (\|\partial_t(\eta_u)\|^2 + \alpha_1^2 \|\partial_t(\nabla \eta_u)\|^2) dt + \frac{s}{2\Delta t} \int_{t^n}^{t^{n+1}} (\|\partial_t(\eta_B)\|^2 + \alpha_2^2 \|\partial_t(\nabla \eta_B)\|^2) dt \\
& \quad + \frac{\alpha_1^2}{2} \left\| \nabla \phi_h^{n+\frac{1}{2}} \right\|^2 + \frac{s\alpha_2^2}{2} \left\| \nabla \psi_h^{n+\frac{1}{2}} \right\|^2 + \left(\frac{Re_m^{-1}}{2} \right) \left\| \nabla \eta_u^{n+\frac{1}{2}} \right\|^2 + \left(\frac{sRe_m^{-1}}{2} \right) \left\| \nabla \eta_B^{n+\frac{1}{2}} \right\|^2 \\
& \quad + C(s) \left(\left\| \phi_h^{n+\frac{1}{2}} \right\|^2 + \left\| \psi_h^{n+\frac{1}{2}} \right\|^2 + \Delta t^4 + \Delta t^4 \alpha_1^4 + \Delta t^4 \alpha_2^4 + \alpha_1^4 + \alpha_2^4 + \left\| \eta_u^{n+\frac{1}{2}} \right\|^2 + \left\| \nabla u_h^{n+\frac{1}{2}} \right\|^2 \left\| \nabla \eta_u^{n+\frac{1}{2}} \right\|^2 \right. \\
& \quad \left. + \left\| \nabla B_h^{n+\frac{1}{2}} \right\|^2 \left\| \nabla \eta_B^{n+\frac{1}{2}} \right\|^2 + \left\| \nabla \eta_B^{n+\frac{1}{2}} \right\|^2 + Re_m \left\| \nabla B_h^{n+\frac{1}{2}} \right\|^2 \left\| \nabla \eta_u^{n+\frac{1}{2}} \right\|^2 \right) \quad (4.31)
\end{aligned}$$

Multiplying by $2\Delta t$ and summing over time steps now gives

$$\begin{aligned}
& \|\phi_h^M\|^2 + s \|\psi_h^M\|^2 + \sum_{n=0}^{M-1} \left(Re^{-1} \left\| \nabla \phi_h^{n+\frac{1}{2}} \right\|^2 + s Re_m^{-1} \left\| \nabla \psi_h^{n+\frac{1}{2}} \right\|^2 \right) + \alpha_1^2 \|\nabla \phi_h^M\|^2 + s \alpha_2^2 \|\nabla \psi_h^M\|^2 \\
& \leq C \int_0^T \left(\|\partial_t(\eta_u)\|^2 + \|\partial_t(\nabla \eta_u)\|^2 + s \|\partial_t(\eta_B)\|^2 + s \|\partial_t(\nabla \eta_B)\|^2 \right) dt \\
& + CT(\Delta t^4(1+\alpha_1^4+\alpha_2^4)+\alpha_1^4+\alpha_2^4)+C\Delta t \sum_{n=0}^{M-1} \left(\left\| \nabla \eta_u^{n+\frac{1}{2}} \right\|^2 + \left\| \nabla \eta_B^{n+\frac{1}{2}} \right\|^2 + \left\| \nabla u_h^{n+\frac{1}{2}} \right\|^2 \left\| \nabla \eta_u^{n+\frac{1}{2}} \right\|^2 \right. \\
& \quad \left. + \left\| \nabla B_h^{n+\frac{1}{2}} \right\|^2 \left\| \nabla \eta_B^{n+\frac{1}{2}} \right\|^2 + \left\| \nabla B_h^{n+\frac{1}{2}} \right\|^2 \left\| \nabla \eta_u^{n+\frac{1}{2}} \right\|^2 \right) \\
& + \Delta t C \sum_{n=0}^{M-1} \left(\|\phi_h^{n+1}\|^2 + \alpha_1^2 \|\nabla \phi_h^{n+1}\|^2 + s \|\psi_h^{n+1}\|^2 + s \alpha_2^2 \|\nabla \psi_h^{n+1}\|^2 \right)
\end{aligned} \tag{4.32}$$

Next we use approximation properties of the spaces and the stability estimate, which reduces (4.32) to

$$\begin{aligned}
& \|\phi_h^M\|^2 + s \|\psi_h^M\|^2 + \alpha_1^2 \|\nabla \phi_h^M\|^2 + s \alpha_2^2 \|\nabla \psi_h^M\|^2 \\
& + \Delta t \sum_{n=0}^{M-1} \left(Re^{-1} \left\| \nabla \phi_h^{n+\frac{1}{2}} \right\|^2 + s Re_m^{-1} \left\| \nabla \psi_h^{n+\frac{1}{2}} \right\|^2 \right) \leq C(\Delta t^4 + \Delta t^4 \alpha_1^4 + \Delta t^4 \alpha_2^4 + h^{2k}) \\
& + \Delta t C \sum_{n=0}^{M-1} \left(\|\phi_h^{n+1}\|^2 + \|\psi_h^{n+1}\|^2 + \alpha_1^2 \|\nabla \phi_h^{n+1}\|^2 + s \alpha_2^2 \|\nabla \psi_h^{n+1}\|^2 \right)
\end{aligned} \tag{4.33}$$

Applying the Grönwall inequality followed by the triangle inequality completes the proof. \square

4.2 Numerical tests for MHD-Voigt

We run two numerical experiments to demonstrate the effectiveness of the regularization for incompressible MHD flows. The first is for channel flow over a step, and the second is for predicting current sheets in ideal MHD.

4.2.1 MHD channel flow over a step

For our first MHD experiment, we consider a variation of the benchmark problem of channel flow over a step found in [6, 10, 29]. The parameters of the test problem are: $Re = 500$, $Re_m = 1$, $s = 0.05$, and end-time $T = 50$. The initial condition is to start from rest and without a magnetic field. For time $t > 0$, the velocity inflow is prescribed a constant inflow profile, and an outflow boundary condition is enforced. No slip boundary conditions are enforced for the velocity on the walls of the channel. The magnetic field boundary condition is set to be $B_{\partial\Omega} = \langle 0, 1 \rangle$ on all boundaries. A schematic of the problem setup is shown in Figure 6.

We compute a DNS for the flow up to $T=10$, using the scheme (4.5a)-(4.5d) with $\alpha_1 = \alpha_2 = 0$ and (P_2, P_1^{disc}) SV elements on a barycenter refined Delaunay mesh that

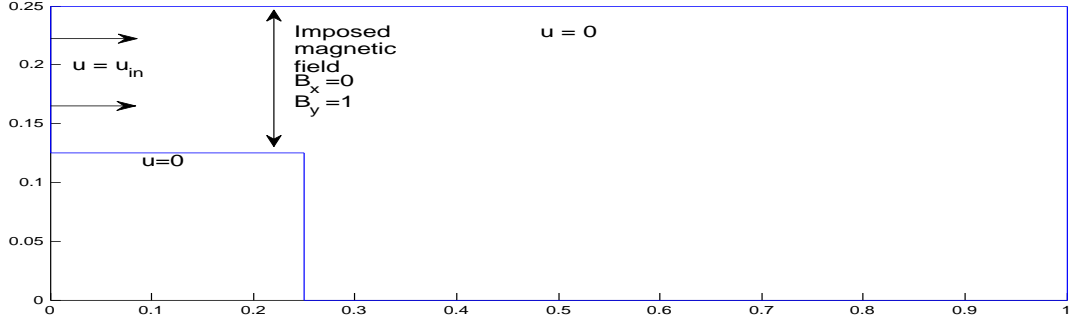


Figure 6: The domain and boundary conditions for the MHD channel flow simulation.

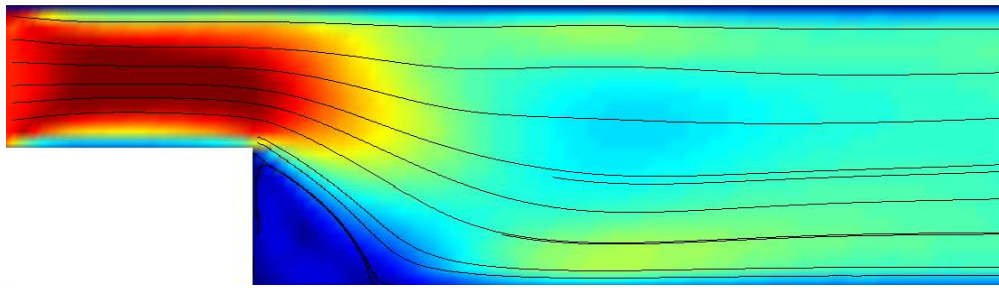


Figure 7: The velocity field as streamlines over speed contours for the resolved MHD channel flow solution, found using a fine mesh and DNS $\alpha_1 = \alpha_2 = 0$.

provides 102,650 degrees of freedom, and a time step of $\Delta t = 0.01$. A plot of the velocity field is shown in Figure 7, and this agrees with the expected physical behavior [6, 10, 29].

We also compute on a much coarser discretization, as it is the goal of a fluid flow model to get an accurate (in some sense) answer on a coarse mesh than is needed by a DNS. We again use (P_2, P_1^{disc}) SV elements, but here we use a much coarser barycenter refined Delaunay mesh that provided 8,666 degrees of freedom and a time step of $\Delta t = 0.1$. The velocity solution of the DNS ($\alpha_1 = \alpha_2 = 0$) is shown in Figure 8, and oscillations are clearly visible in the solution. The Voigt regularization, on the other hand, with $\alpha_1 = \alpha_2 = 0.05$ is able to give a smooth and qualitatively accurate solution using this coarse discretization.

4.2.2 Orszag-Tang vortex

For our final experiment, we repeat a calculation done by J.-G Liu and W. Wang in [24], Friedel et al. in [9], and the authors in [4], known as the incompressible Orszag-Tang vortex problem for MHD. This test problem is for ideal 2D MHD, with $Re = Re_m = \infty$, $f = \nabla \times g = 0$, $s = 1$, and on the 2π periodic box with initial condition

$$u_0 = < -\sin(y + 2), \sin(x + 1.4) >^T \quad B_0 = < -\frac{1}{3} \sin(y + 6.2), \frac{2}{3} \sin(2x + 2.3) >^T.$$

The solution is known to develop singularity-like structures known as current sheets, where the current density grows exponentially in time, and the thickness of the sheet shrinks at an exponential rate. By $T=2.7$, the formation of the sheets is known to occur, and can be seen in the contour plot of $\nabla \times B$ (which is a scalar in 2D).

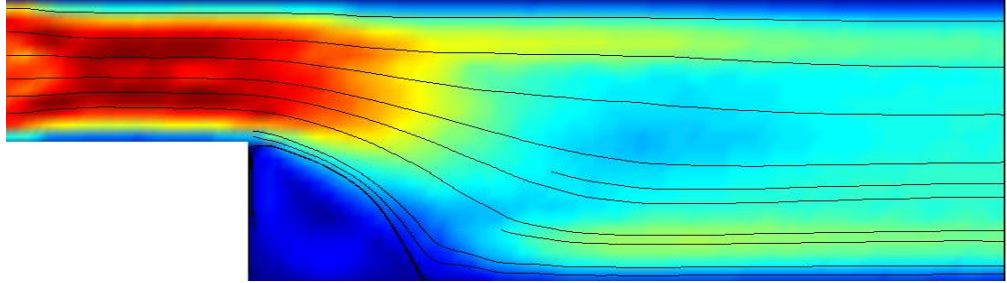


Figure 8: The velocity solution as streamlines over speed contours, found using a DNS ($\alpha_1 = \alpha_2 = 0$) on a coarse mesh.

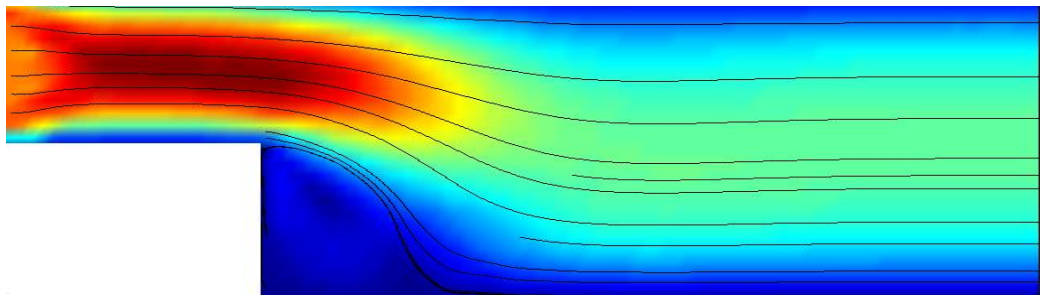


Figure 9: The velocity solution as streamlines over speed contours, found using the Voigt regularization ($\alpha_1 = 0.05$, $\alpha_2 = 0.05$) on a coarse mesh.

We compute with the scheme (4.5a)-(4.5d) using (P_2, P_1^{disc}) SV elements on a barycenter refinement of a uniform triangulation of $(-\pi, \pi)^2$. We first compute a reference solution on a fine mesh that provides 345,092 total degrees of freedom, with a time step of $\Delta t = 0.01$, up to $T=2.7$. A plot of the current density at $T=2.7$ for this solution is shown in Figure 10. This solution agrees well with the results in [4, 9, 24].

We next compute on a coarser mesh, again with (P_2, P_1^{disc}) SV elements on a barycenter refinement of a uniform triangulation of $(-\pi, \pi)^2$, which provides 15,748 total degrees of freedom. Again we use a timestep of $\Delta t = 0.01$ to compute up to $T=2.7$. Solutions are found on these coarse mesh computations in several minutes, while the fine mesh computations take several hours. We test this problem on the coarse mesh with no model ($\alpha_1 = \alpha_2 = 0$), and $\alpha_1=0.1 \approx h$ with $\alpha_2=0.1, 0.05, 0.01, 0.001$, and 0. Varying α_2 's are used because the true solution exhibits singular behavior in its magnetic field, and thus ‘too much’ regularization of the magnetic field can over-smooth and not allow a correct prediction by the model. We note that the idea of using the Voigt regularization only in the momentum equation in MHD was previously studied analytically in [5, 18], and found to be well-posed.

The coarse mesh results are shown in Figure 11 as current density contour plots at $T = 2.7$. and we observe that ‘no model’ gives an under resolved solution as it is unable to predict the current sheets in the bottom right corner. For the MHD-Voigt solution, we observe that with $\alpha_2=0.1, 0.05$ and 0.01, current sheets are found in approximately the right places, but their magnitude is too small. However, the MHD-Voigt solutions with $\alpha_2=0.001$ and 0 find good approximations of the true solution, finding current sheets in the right places and with the right magnitude. Hence we conclude that by taking α_2 too large

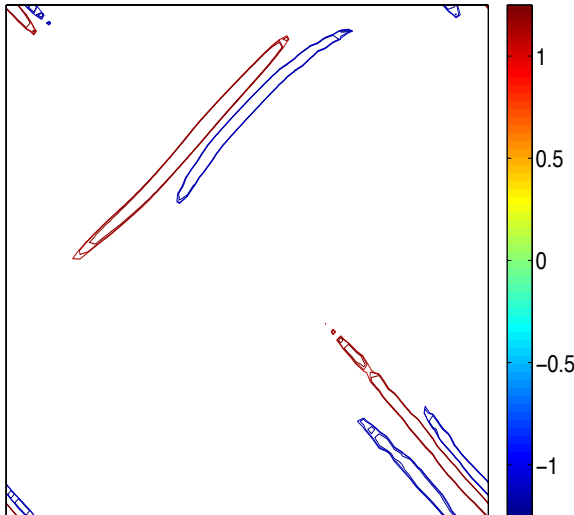


Figure 10: The current density of the fine mesh solution $\nabla \times B$ at $T=2.7$.

in this problem had a significant over-regularizing effect in this problem, but taking $\alpha_2 = 0$ provides a good coarse mesh approximation.

5 Conclusion

We studied finite element algorithms for the NSE-Voigt and MHD-Voigt regularizations. Both algorithms are proven to be unconditionally stable with respect to time step, and optimally convergent if the regularization parameters are chosen $\alpha_1, \alpha_2 \leq \min\{\Delta t, h^{k/2}\}$, where k is the degree of the velocity approximating polynomial (so $k = 2$ is the most common choice). Several numerical examples are provided that show for both NSE and MHD, the Voigt regularization can provide better coarse mesh approximations to the physical solution than can direct computations of NSE and MHD, in that correct qualitative behavior can be captured and spurious oscillations significantly damped. Finally, our MHD test for the Orszag-Tang vortex problem showed that the MHD-Voigt model can be altered so that it can predict flows with singular behavior in the magnetic field, by using the Voigt regularization only in the momentum equation; this is an interesting phenomena that the authors plan to consider in future work. Furthermore, this result suggests there may also be problems where regularization is only necessary in the induction equation and not in the momentum equation.

References

- [1] G. Baker. Galerkin approximations for the Navier-Stokes equations. Harvard University, August 1976.
- [2] Y. Cao, E. Lunasin, and E. S. Titi. Global well-posedness of the three-dimensional viscous and inviscid simplified Bardina turbulence models. *Commun. Math. Sci.*, 4(4):823–848, 2006.

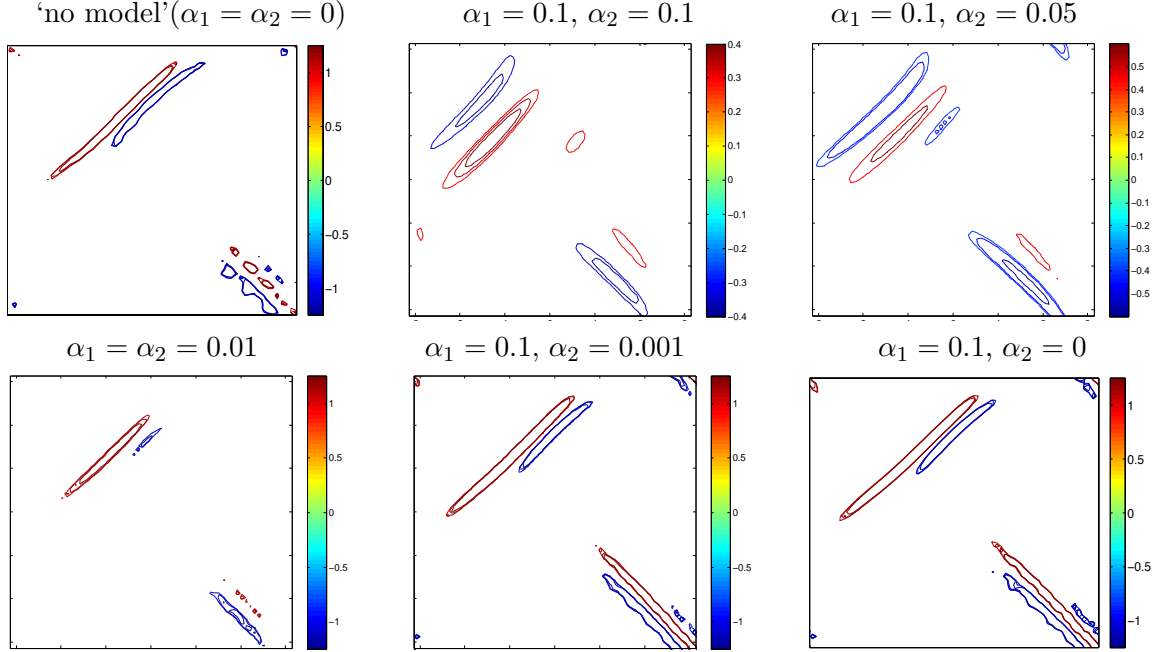


Figure 11: The current density of the coarse mesh solutions $\nabla \times B$ at $T=2.7$ for (top left) MHD without regularization, and for MHD-Voigt with varying regularization parameter α_2 .

- [3] M. Case, V. Ervin, A. Linke, and L. Rebholz. Improving mass conservation in FE approximations of the Navier Stokes equations using C^0 velocity fields: A connection between grad-div stabilization and Scott-Vogelius elements. *SIAM Journal on Numerical Analysis*, 49(4):1461–1481, 2011.
- [4] M. Case, A. Labovsky, L. Rebholz, and N. Wilson. A high physical accuracy method for incompressible magnetohydrodynamics. *International Journal on Numerical Analysis and Modeling, Series B*, 1(2):219–238, 2010.
- [5] D. Catania and P. Secchi. Global existence for two regularized MHD models in three space-dimension. *Portugaliae Mathematica*, 68(1):41–52, 2011.
- [6] R. Codina and N. Silva. Stabilized finite element approximation to the stationary magnetohydrodynamics equations. *Computational Mechanics*, 194:334–355, 2006.
- [7] P. Davidson. *An Introduction to Magnetohydrodynamics*. Cambridge, 2001.
- [8] L. Davis and F. Pahlevani. Semi-implicit schemes for transient Navier-Stokes equations and eddy viscosity models. *Numerical Methods for Partial Differential Equations*, 25:212–231, 2009.
- [9] H. Friedel, R. Grauer, and C. Marliani. Adaptive mesh refinement for singular current sheets in incompressible magnetohydrodynamic flows. *Journal of Computational Physics*, 134:190–198, 1997.
- [10] J. Gerbeau. A stabilized finite element method for the incompressible magnetohydrodynamic equation. *Numerische Mathematik*, 87:83–111, 2000.

- [11] M. Gunzburger, O. Ladyzhenskaya, and J. Peterson. On the global unique solvability of initial-boundary value problems for the coupled modified Navier-Stokes and Maxwell equations. *J. Math. Fluid Mech.*, 6:462–482, 2004.
- [12] M. Gunzburger and C. Trenchea. Analysis and discretization of an optimal control problem for the time-periodic MHD equations. *J. Math Anal. Appl.*, 308(2):440–466, 2005.
- [13] M. Gunzburger and C. Trenchea. Analysis of optimal control problem for three-dimensional coupled modified Navier-Stokes and Maxwell equations. *J. Math Anal. Appl.*, 333:295–310, 2007.
- [14] J. Heywood and R. Rannacher. Finite element approximation of the nonstationary Navier-Stokes problem. Part IV: Error analysis for the second order time discretization. *SIAM J. Numer. Anal.*, 2:353–384, 1990.
- [15] J. Heywood, R. Rannacher, and S. Turek. Artificial boundaries and flux and pressure conditions for the incompressible Navier-Stokes equations. *International Journal for Numerical Methods in Fluids*, 22:325–352, 1996.
- [16] A. Labovsky, W. Layton, C. Manica, M. Neda, and L. Rebholz. The stabilized extrapolated trapezoidal finite element method for the Navier-Stokes equations. *Comput. Methods Appl. Mech. Engrg.*, 198:958–974, 2009.
- [17] A. Larios and E. S. Titi. On the higher-order global regularity of the inviscid Voigt-regularization of three-dimensional hydrodynamic models. *Discrete Contin. Dyn. Syst. Ser. B*, 14(2/3 #15):603–627, 2010.
- [18] A. Larios and E. S. Titi. Higher-order global regularity of an inviscid Voigt-regularization of the three-dimensional inviscid resistive magnetohydrodynamic equations. *arXiv:1104.0358*, 2012. (in submission).
- [19] A. Larios, B. Wingate, M. Petersen, and E. S. Titi. Numerical analysis of the Euler-Voigt equations and a numerical investigation of the finite-time blow-up of solutions. (in preparation).
- [20] W. Layton. *An introduction to the numerical analysis of viscous incompressible flows*. SIAM, 2008.
- [21] B. Levant, F. Ramos, and E. S. Titi. On the statistical properties of the 3d incompressible Navier-Stokes-Voigt model. *Commun. Math. Sci.*, 8(1):277–293, 2010.
- [22] A. Linke. Collision in a cross-shaped domain — A steady 2d Navier-Stokes example demonstrating the importance of mass conservation in CFD. *Comp. Meth. Appl. Mech. Eng.*, 198(41–44):3278–3286, 2009.
- [23] J.-G. Liu and R. Pego. Stable discretization of magnetohydrodynamics in bounded domains. *Commun. Math. Sci.*, 8(1):234–251, 2010.
- [24] J-G.. Liu and W. Wang. Energy and helicity preserving schemes for hydro and magnetohydro-dynamics flows with symmetry. *J. Comput. Phys.*, 200:8–33, 2004.

- [25] A. P. Oskolkov. The uniqueness and solvability in the large of boundary value problems for the equations of motion of aqueous solutions of polymers. *Zap. Naučn. Sem. Leningrad. Otdel. Mat. Inst. Steklov. (LOMI)*, 38:98–136, 1973. Boundary value problems of mathematical physics and related questions in the theory of functions, 7.
- [26] A. P. Oskolkov. On the theory of unsteady flows of Kelvin-Voigt fluids. *Zap. Nauchn. Sem. Leningrad. Otdel. Mat. Inst. Steklov. (LOMI)*, 115:191–202, 310, 1982. Boundary value problems of mathematical physics and related questions in the theory of functions, 14.
- [27] J. Qin. *On the convergence of some low order mixed finite elements for incompressible fluids*. PhD thesis, Pennsylvania State University, 1994.
- [28] R. Temam. *Navier-Stokes Equations, Theory and Numerical Analysis*, volume 2. North-Holland Publishing Company, 1979.
- [29] N. Wilson. On the Leray-deconvolution model for the incompressible magnetohydrodynamics equations. *Applied Mathematics and Computation*, to appear, 2012.
- [30] S. Zhang. A new family of stable mixed finite elements for the 3d Stokes equations. *Mathematics of Computation*, 74:543–554, 2005.
- [31] S. Zhang. On the P1 Powell-Sabin divergence-free finite element for the Stokes equations. *J. Comput. Math.*, 26(3):456–470, 2008.
- [32] S. Zhang. Divergence-free finite elements on tetrahedral grids for $k \geq 6$. *Math. Comp.*, 80(274):669–695, 2011.
- [33] S. Zhang. Quadratic divergence-free finite elements on Powell-Sabin tetrahedral grids. *Calcolo*, 48(3):211–244, 2011.